Journal of the Society of Automotive Engineers Malaysia
Volume 5, Issue 4 (Special Issue), pp 75-88, October 2021
e-ISSN 2550-2239 & ISSN 2600-8092

A Comparison Study on Functions for Lane Change Path in Emergency Obstacle Avoidance

A. S. P. Singh[*1,2], A. Putra[1,2] and K. A. Abu Kassim[3]

[1]Mechanical Engineering Faculty, Universiti Teknikal Malaysia Melaka,
Hang Tuah Jaya, 76100 Durian Tunggal, Melaka, Malaysia
[2]Centre for Advanced Research on Energy, Universiti Teknikal Malaysia Melaka,
Hang Tuah Jaya, 76100 Durian Tunggal, Melaka, Malaysia
[3]Malaysian Institute of Road Safety Research (MIROS), 43000 Kajang, Selangor, Malaysia

[*]*Corresponding author: amriksingh@utem.edu.my*

ORIGINAL ARTICLE **Open Access**

Article History:

Received
15 Oct 2020

Accepted
29 Aug 2021

Available online
1 Oct 2021

Abstract – *In situations in which autonomous emergency braking is ineffective in avoiding an obstacle encountered in the current lane, autonomous emergency steering may be useful in avoiding the obstacle. This paper focuses on the comparison of the lane change paths by using autonomous emergency steering. Six functions that are considered for the generation of the desired lane change path are circular arcs, ramp sinusoidal, polynomial, clothoid, trapezoidal acceleration profile, and sigmoid. The longitudinal distance required to avoid the obstacle which is the total longitudinal distance for the complete lane change is calculated for different vehicle speeds and tire-road friction coefficients. The distances obtained for the six functions are compared and the function that achieves the shortest longitudinal distance to avoid the obstacle is regarded as the most effective function. For a total lateral displacement of 3.5 m and friction coefficients of 0.9, 0.5, and 0.2, circular arcs give the shortest and clothoid gives the longest longitudinal distance required to avoid the obstacle.*

Keywords: Autonomous vehicle, braking, collision avoidance, lane change, steering

Journal homepage: www.jsaem.my

1.0 INTRODUCTION

Autonomous vehicles are required to execute autonomous maneuvers including those forcing the vehicle to operate at the friction limits (Fors et al., 2020). Autonomous collision avoidance (Yokoyama et al., 2018), autonomous drifting (Goh et al., 2020), and autonomous racing (Kapania & Gerdes, 2020) are among the autonomous maneuvers in which the vehicle is operated at the friction limits. Autonomous collision avoidance is an important function of autonomous vehicles. In previous studies, different collision avoidance problems have been studied. Among them are obstacle avoidance (Singh & Nishihara, 2020), unintended road departure (Alleyne, 1997), collision avoidance in an intersection (Arikere et al., 2019), collision

avoidance in overtaking maneuvers (Isermann et al., 2012), and post-impact collision avoidance (Yang et al., 2014).

In this paper, the scenario in which a vehicle encounters a stationary obstacle in the current lane is considered. This obstacle may be avoided by using either a stopping or lane change maneuver. For low vehicle speed, the stopping maneuver is more effective compared to the lane change maneuver because it requires a shorter stopping distance compared to the longitudinal distance required for the complete lane change. For high vehicle speed, a lane change maneuver is more effective compared to a stopping maneuver because a lane change maneuver requires a shorter longitudinal distance for the complete lane change compared to the stopping distance.

The emergency lane change maneuver can be realized by using either steering (Shah et al., 2015; Soudbakhsh et al., 2013) or combined steering and braking (Yuan et al., 2019; Gao et al., 2019; Singh & Nishihara, 2018). One of the common approaches for autonomous lane change maneuver is first, a desired path or trajectory for lane change is generated and then, this desired path or trajectory is tracked by using either steering or steering with braking. Simple functions are desired for the generation of the desired lane change paths compared to the approaches that require iterative solutions. Examples of the functions that are used for desired lane change path generation are polynomial (Shah et al., 2015), ramp sinusoidal (Sledge & Marshek, 1997; Singh et al., 2020), and clothoid (Funke & Gerdes, 2016). These functions take into account the vehicle speed, friction limit, and total lateral displacement for the generation of the desired lane change path. Functions like sigmoid and trapezoidal acceleration profiles consider the maximum lateral jerk in addition to vehicle speed, friction limit, and total lateral displacement to generate the desired lane change path. The maximum lateral jerk is limited by the maximum steering rate.

In this paper, six functions that are considered for the generation of the desired path for emergency lane change are circular arcs, ramp sinusoidal, polynomial, clothoid, trapezoidal acceleration profile, and sigmoid. The objective of this study is to determine which of these functions would achieve the shortest longitudinal distance to avoid the obstacle. The longitudinal distance required to avoid the obstacle is calculated for different vehicle speeds and tire-road friction coefficients. Besides, the regions on the vehicle speed–friction coefficient plane in which either the stopping or lane change maneuver is more effective are presented.

This paper is organized as follows. The obstacle avoidance problem and maneuvers for obstacle avoidance are introduced in the next section. In the third section, the functions that are used to generate the desired lane change path are described. Numerical examples are provided in the fourth section. The last section concludes the paper.

2.0 OBSTACLE AVOIDANCE PROBLEM AND MANEUVERS

The collision avoidance problem considered in this paper is one in which a vehicle traveling on a straight road suddenly encounters a stationary obstacle in the current lane. The two avoidance maneuvers considered are the stopping and lane-change maneuvers. For each maneuver, the longitudinal distance required to avoid the obstacle is determined and used to decide if a collision is avoidable.

Figure 1 shows the stopping maneuver in which a vehicle in blue is traveling with an initial speed of u_x and the vehicle brakes to stop just before the stationary obstacle. The stopping distance S_d, which is the longitudinal distance required to stop the vehicle, is given as

$$S_d = \frac{u_x^2}{2a_{x,\max}} \tag{1}$$

where $a_{x,\max}$ is the maximum longitudinal deceleration. This maximum deceleration is given as

$$a_{x,\max} = \mu g \tag{2}$$

where μ is the tire-road friction coefficient and g is the gravitational acceleration.

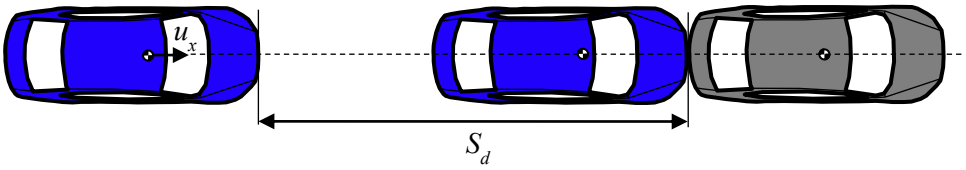

Figure 1: Stopping maneuver

The lane change maneuver is shown in Figure 2 where a vehicle in blue executes a lane change maneuver to avoid a collision with the stationary obstacle. During the lane change maneuver, the vehicle is assumed to be traveling at a constant speed u_x. In Figure 2, L denotes the longitudinal distance required to avoid the obstacle and D_y denotes the total lateral displacement. In the next section, six functions are considered for the generation of the desired lane change paths, and the mathematical equation for the longitudinal distance required to avoid the obstacle for each function is given.

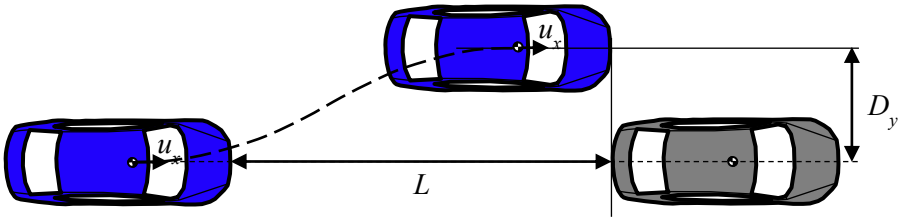

Figure 2: Lane change maneuver

3.0 FUNCTIONS FOR LANE CHANGE PATH GENERATION

In this section, six functions used to generate the desired lane change path are described. These functions are circular arcs, ramp sinusoidal, polynomial, clothoid, trapezoidal acceleration profile, and sigmoid. For the lane change maneuvers considered in this paper, the maximum lateral acceleration $a_{y,\max}$ is limited by the tire-road friction coefficient. The maximum lateral acceleration is written as

$$a_{y,\max} = \mu g \tag{3}$$

where μ is the tire-road friction coefficient and g is the gravitational acceleration. For the trapezoidal acceleration profile and sigmoid functions, in addition to the maximum lateral acceleration, maximum lateral jerk is considered.

3.1 Circular Arcs

Two circular arcs can be used to represent the lane change path (Sledge and Marshek, 1997). The lateral position is given as

$$y(x) = \begin{cases} \rho - \sqrt{\rho^2 - x^2} & ,0 \le x < \dfrac{L_{ca}}{2} \\ D_y - \rho + \sqrt{\rho^2 - x^2 + 2xL_{ca} - L_{ca}^2} & ,\dfrac{L_{ca}}{2} \le x \le L_{ca} \end{cases} \tag{4}$$

where ρ is the constant radius of curvature and is given by

$$\rho = \frac{L_{ca}^2 + D_y^2}{4D_y} \tag{5}$$

and L_{ca} is the total longitudinal distance required for complete lane change. The minimum radius of curvature can be written as

$$\rho_{\min} = \frac{u_x^2}{a_{y,\max}} \tag{6}$$

By substituting Equation (6) into Equation (5), and then by solving the resulting equation for L_{ca}, the total longitudinal distance for lane change is obtained (Sledge & Marshek, 1997)

$$L_{ca} = \sqrt{\frac{4D_y u_x^2}{a_{y,\max}} - D_y^2} \tag{7}$$

3.2 Ramp Sinusoidal

For the generation of the desired lane change paths, the ramp sinusoidal function is preferred over the circular arcs because ramp sinusoidal provides continuous curvature. Sledge and Marshek (1997) provided the following form of the lateral position

$$y(x) = D_y \left[\frac{x}{L_{rs}} - \frac{1}{2\pi} \sin\left(\frac{2\pi x}{L_{rs}} \right) \right] \tag{8}$$

where L_{rs} is the total longitudinal distance for lane change. The minimum radius for Equation (8) is given by Sledge and Marshek (1997) as

$$\rho_{\min} = \frac{L_{rs}^2}{2\pi D_y} \tag{9}$$

As described by Sledge and Marshek (1997), the total longitudinal distance for lane change is obtained by first equating Equations (6) and (9) and then, by solving the resulting equation for L_{rs}

$$L_{rs} = u_x \sqrt{\frac{2\pi D_y}{a_{y,\max}}} \tag{10}$$

3.3 Polynomial

A quintic polynomial can be used to represent the lane change path. The quintic polynomial is given as

$$y(x) = a_5 x^5 + a_4 x^4 + a_3 x^3 + a_2 x^2 + a_1 x + a_0 \tag{11}$$

The polynomial coefficients a_5 to a_0 as in Equation (11) must satisfy the following constraints (Nelson, 1989):

$$y = 0, \quad \frac{dy}{dx} = 0, \quad K = 0 \quad \text{at } x = 0 \tag{12}$$

$$y = D_y, \quad \frac{dy}{dx} = 0, \quad K = 0 \text{ at } x = L_p \tag{13}$$

where K denotes the curvature of $y(x)$ and is written as

$$K = \frac{\frac{d^2y}{dx^2}}{\left[1 + \left(\frac{dy}{dx}\right)^2\right]^{\frac{3}{2}}} \tag{14}$$

The quintic polynomial that satisfies the constraints in Equations (12) and (13) is written as given by Nelson (1989)

$$y(x) = D_y \left[10\left(\frac{x}{L_p}\right)^3 - 15\left(\frac{x}{L_p}\right)^4 + 6\left(\frac{x}{L_p}\right)^5\right] \tag{15}$$

The total longitudinal distance for lane change is given by Weber (2012) as

$$L_p = u_x \sqrt{\frac{10 D_y}{\sqrt{3} a_{y,\max}}} \tag{16}$$

3.4 Clothoid

Clothoid is defined as a curve with a curvature that varies linearly with the distance traveled along the curve. Clothoids are widely used in road designs and for lane change paths (Funke & Gerdes, 2016; Wilde, 2009; Gray et al., 2012). The curvature K is written as

$$K(s) = \alpha s \tag{17}$$

where α is the sharpness or the rate of change of the curvature with respect to the distance s traveled along the curve. Figure 3 shows a clothoid profile that consists of four clothoids to form a desired lane-change path. In Figure 3, l is the total distance traveled along the lane change path and $K_{\max}$ is the maximum curvature. The total longitudinal distance for lane change

L_c is determined by considering the friction limit and the details on this are given by Funke and Gerdes (2016).

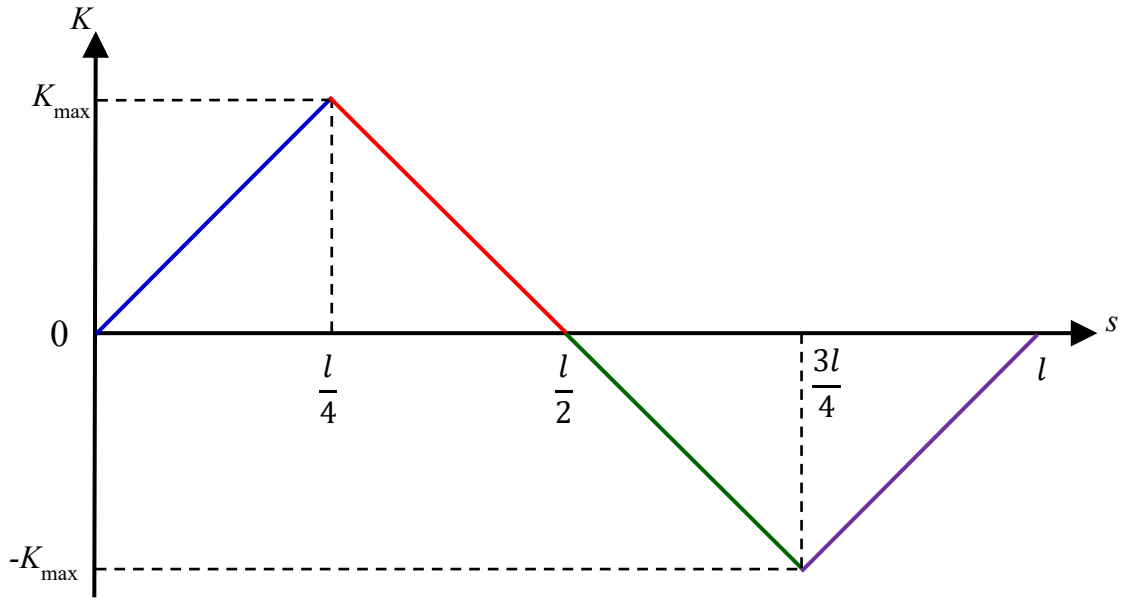

Figure 3: Clothoid profile for lane change

3.5 Trapezoidal Acceleration Profile

The trapezoidal acceleration profile (TAP) that assumes a trapezoidal form for lateral acceleration is used to generate a lane change path is shown in Figure 4. In Figure 4, the blue line represents the maximum lateral jerk and the red line represents the maximum lateral acceleration. In previous studies, trapezoidal acceleration profile-based lane change paths are considered in studies on automated highways systems (Chee & Tomizuka, 1994) and collision avoidance (Soudbakhsh et al., 2013).

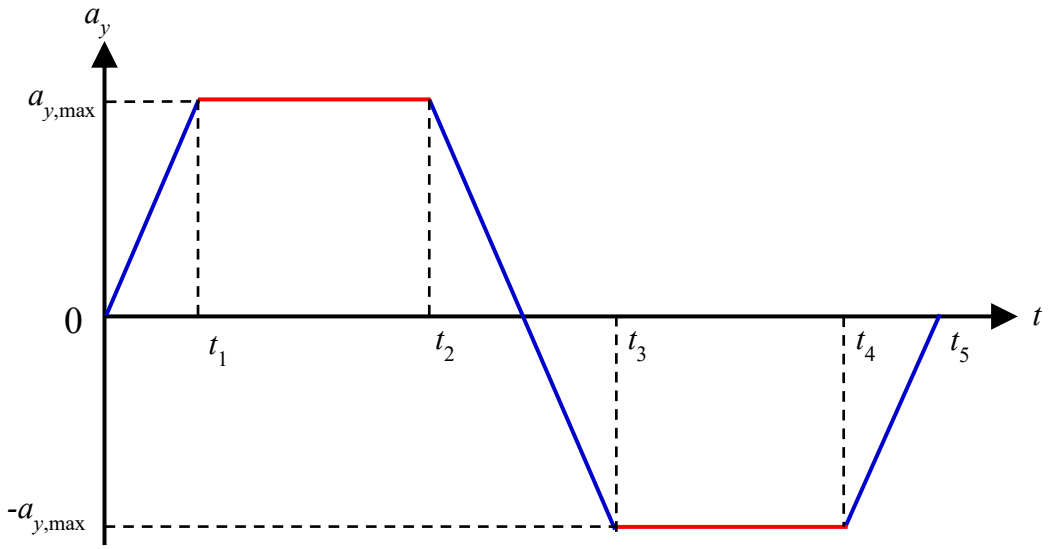

Figure 4: Trapezoidal acceleration profile for lane change

The parameters t_1, t_2, t_3, t_4, and t_5 (Chee & Tomizuka, 1994) are given as

$$t_1 = \frac{a_{y,\max}}{J_{y,\max}} \tag{18}$$

$$t_2 = \frac{-t_1^2 + \sqrt{t_1^4 + 4t_1 \frac{D_y}{J_{y,\max}}}}{2t_1} \tag{19}$$

$$t_3 = 2t_1 + t_2 \tag{20}$$

$$t_4 = t_1 + 2t_2 \tag{21}$$

$$t_5 = 2t_1 + 2t_2 \tag{22}$$

where $a_{y,\max}$ is the maximum lateral acceleration, $J_{y,\max}$ is the maximum lateral jerk, and t_5 is the time required to complete the lane change. The lateral position for the lane change path can be obtained by integrating the desired lateral acceleration twice with respect to time. The total longitudinal distance for lane change L_{tap} is determined by setting appropriate values for the maximum lateral acceleration and maximum lateral jerk. The distance L_{tap} is written as

$$L_{tap} = u_x t_5 \tag{23}$$

3.6 Sigmoid

A sigmoid function is used by Isermann et al. (2008) to represent the lane change path for collision avoidance study. The lateral position during the lane change is given as

$$y(x) = \frac{D_y}{1 + e^{-b(x-c)}} \tag{24}$$

where b is the slope of the sigmoid and c is half of the total longitudinal distance for lane change L_s. The parameters b and c are determined by considering the maximum lateral acceleration and maximum lateral jerk. Once c is determined, the longitudinal distance required to avoid the obstacle can be calculated by using

$$L_s = 2c \tag{25}$$

The details on the determination of b and c are given by Arbitmann et al. (2012).

4.0 NUMERICAL EXAMPLES

In this section, the total longitudinal distances for lane change for the six functions as described in the previous section are computed and compared. In all examples, the total lateral displacement D_y is assumed to be 3.5 m. Figures 5 to 7 show the longitudinal distance required to avoid the obstacle as a function of vehicle speed for friction coefficients of 0.9, 0.5, and 0.2, respectively. In these figures, the black line represents the stopping maneuver, and the blue, red, green, purple, gray, and cyan lines represent the lane change maneuvers by using circular arcs, ramp sinusoidal, polynomial, clothoid, trapezoidal acceleration profile, and sigmoid functions, respectively. The intersection point between the stopping and lane-change maneuvers is a point where the stopping distance and total longitudinal distance for lane change are the same.

For the case in which the friction coefficient is equal to 0.9, the functions can be arranged from the shortest to the longest longitudinal distance required to avoid the obstacle as circular arcs, polynomial, ramp sinusoidal, trapezoidal acceleration profile, sigmoid, and clothoid. It is apparent from Figure 5 that the longitudinal distances required to avoid the obstacle using the ramp sinusoidal and trapezoidal acceleration profile are near to each other.

Figure 6 shows the longitudinal distance required to avoid the obstacle as a function of vehicle speed for a total lateral displacement of 3.5 m and a friction coefficient of 0.5. The functions that give the shortest to the longest longitudinal distance required to avoid the obstacle, in order are circular arcs, trapezoidal acceleration profile, polynomial, ramp sinusoidal, sigmoid, and clothoid. The longitudinal distance required to avoid the obstacle as a function of vehicle speed for total lateral displacement of 3.5 m and a friction coefficient of 0.2 is shown in Figure 7. In this case, the functions arranged according to the longitudinal distance required to avoid the obstacle from shortest to longest, in order are circular arcs, trapezoidal acceleration profile, polynomial, ramp sinusoidal, sigmoid, and clothoid.

As can be seen in Figures 5 to 7, for a given friction coefficient, the longitudinal distance required to avoid the obstacle increases with vehicle speed. For the three friction coefficients (0.9, 0.5, and 0.2), circular arcs give the shortest and clothoid gives the longest longitudinal distance to avoid the obstacle.

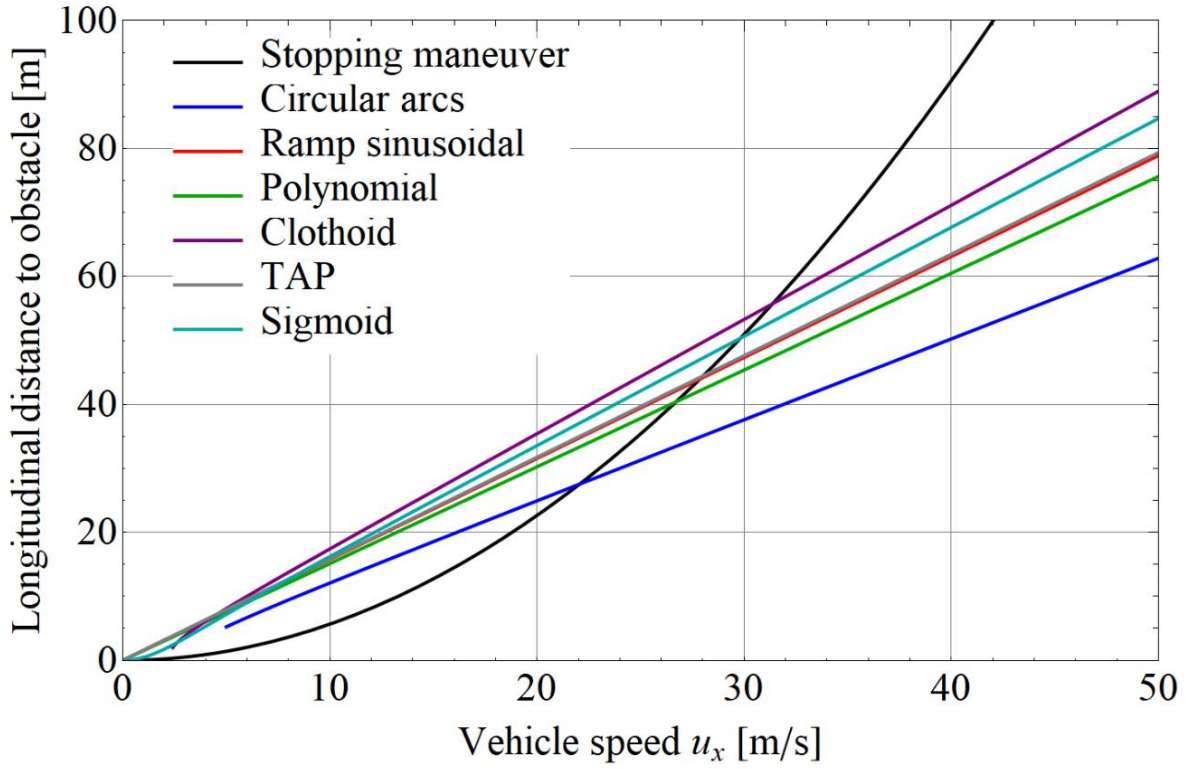

Figure 5: Longitudinal distance required to avoid the obstacle as a function of vehicle speed assuming a total lateral displacement of 3.5 m and a friction coefficient of 0.9

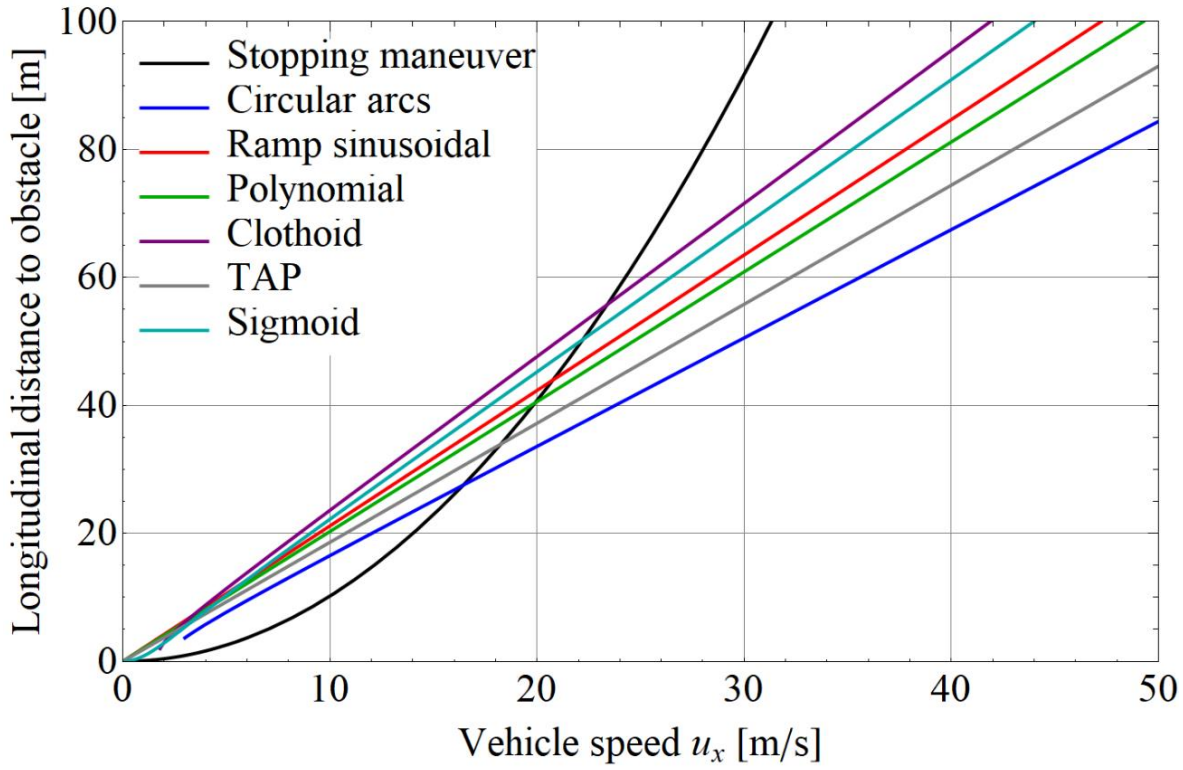

Figure 6: Longitudinal distance required to avoid the obstacle as a function of vehicle speed assuming a total lateral displacement of 3.5 m and a friction coefficient of 0.5

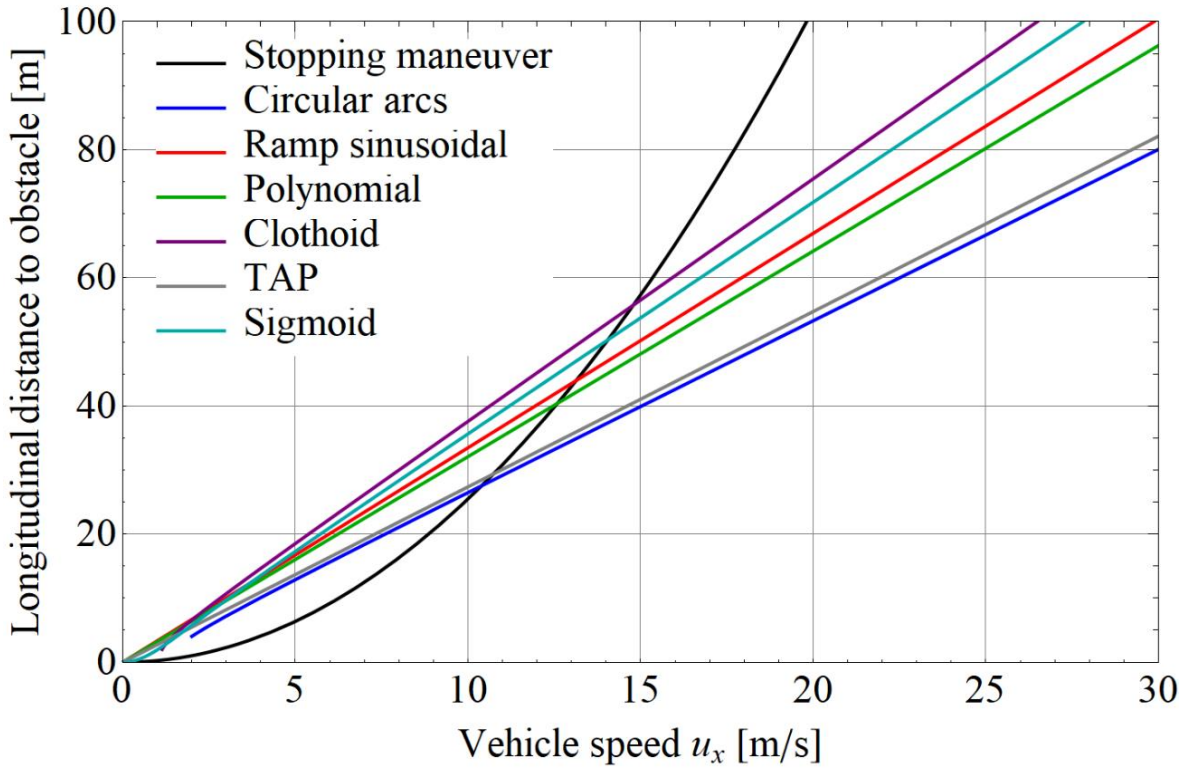

Figure 7: Longitudinal distance required to avoid the obstacle as a function of vehicle speed assuming a total lateral displacement of 3.5 m and a friction coefficient of 0.2

Figures 8(a), 8(b), 8(c), 8(e), and 8(f) show the contour plots of the total longitudinal distance for lane change using circular arcs, ramp sinusoidal, polynomial, trapezoidal acceleration profile, and sigmoid, respectively. It can be seen that the shortest total longitudinal distance for lane change is achieved when the vehicle speed is low and the friction coefficient is high. For a given vehicle speed, a shorter total longitudinal distance for lane change is achievable at high friction because the maximum available acceleration is used to perform the lane change maneuver. Figure 8(d) shows the contour plot of the maximum entry vehicle speed for lane change using clothoid. As shown in Figure 8(d), the highest maximum entry vehicle speed is obtained at a long longitudinal distance to the obstacle and high friction coefficient.

The regions in which either stopping or lane change maneuver is more effective are shown in Figure 9. In Figure 9(a), the red region is where the longitudinal distance required to avoid the obstacle by stopping maneuver is shorter than that is obtained by lane change maneuver using circular arcs and the blue region is where the longitudinal distance required to avoid the obstacle by lane change maneuver using circular arcs is shorter than that is obtained by stopping maneuver. The maneuver that gives the shortest longitudinal distance to avoid the obstacle is considered the most effective maneuver. Similar explanations can be made for Figures 9(b), 9(c), 9(e) and 9(f). The red region in Figure 9(d) indicates that the maximum entry speed obtained by stopping maneuver is higher than that is obtained by lane change maneuver using clothoid and the blue region indicates that the maximum entry speed by lane change maneuver using clothoid is higher than that is obtained using stopping maneuver. The maneuver that gives the highest entry maximum vehicle speed is considered the most effective maneuver.

Singh et al. (2021) compared the time to collision for lane changes generated by using circular arcs, ramp sinusoidal, polynomial, trapezoidal acceleration profile, and sigmoid. Time to collision is another collision avoidance index. A study by Singh and Nishihara (2021) presented dimensionless versions of the longitudinal distance to obstacle and time to collision for the desired lane change path generated by using the polynomial function.

5.0 CONCLUSION

In this paper, six functions are considered for the generation of the desired lane change paths. These functions are compared in terms of the total longitudinal distance for lane change which represents the longitudinal distance required to avoid the obstacle. For a given total lateral displacement and friction coefficients of 0.9, 0.5, and 0.2, the shortest and longest longitudinal distances required to avoid the obstacle are obtained by using circular arcs and clothoid, respectively. At low vehicle speed, the stopping maneuver requires a shorter avoidance distance compared to the lane change maneuver and vice versa. The regions on vehicle speed-friction coefficient plane in which either braking or lane change maneuver requires the shorter avoidance distance are identified.

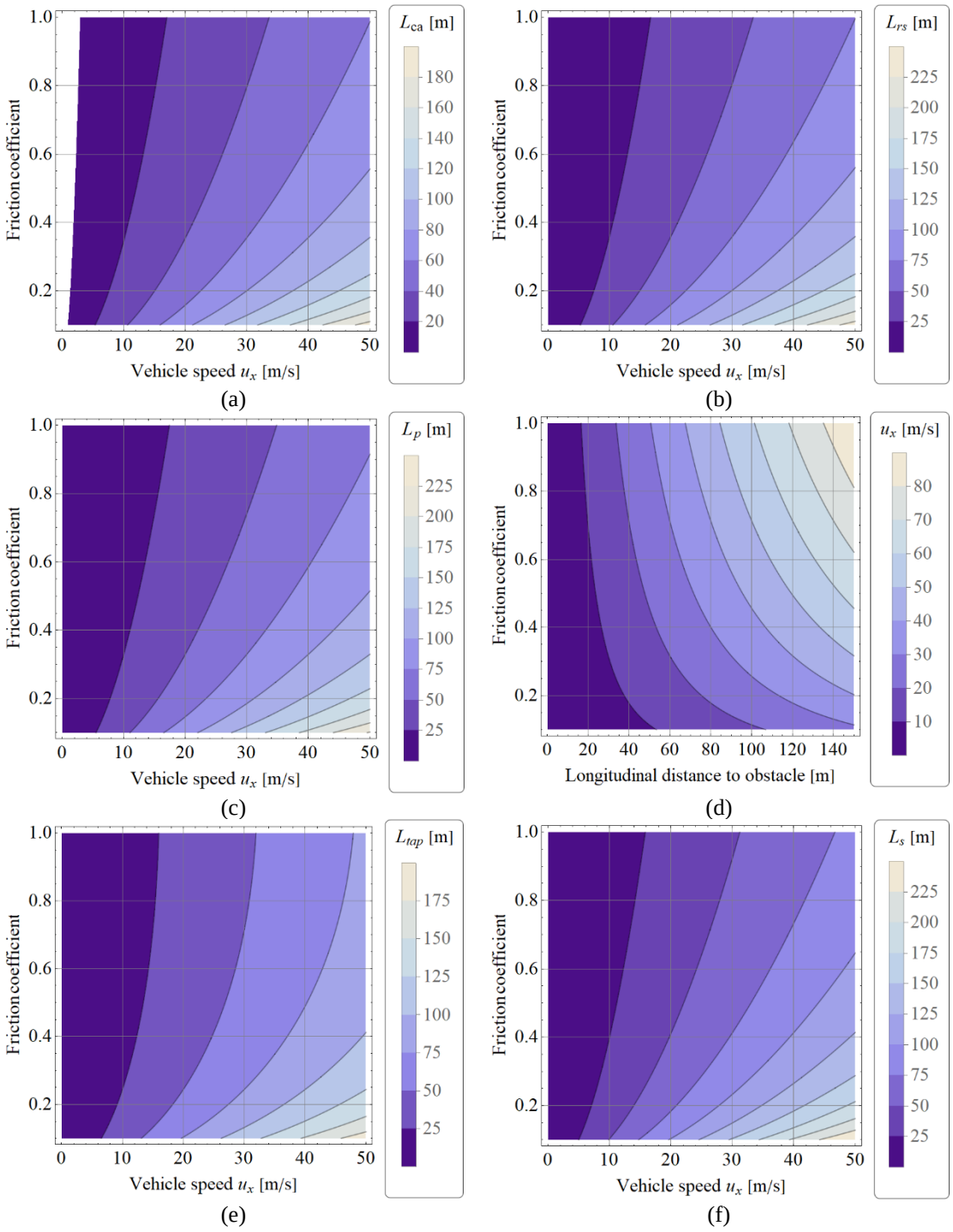

Figure 8: Contour plot of the total longitudinal distance for lane change for (a) circular arcs, (b) ramp sinusoidal, (c) polynomial, (e) trapezoidal acceleration profile, and (f) sigmoid, and contour plot of the maximum entry vehicle speed for (d) clothoid assuming a total lateral displacement of 3.5 m

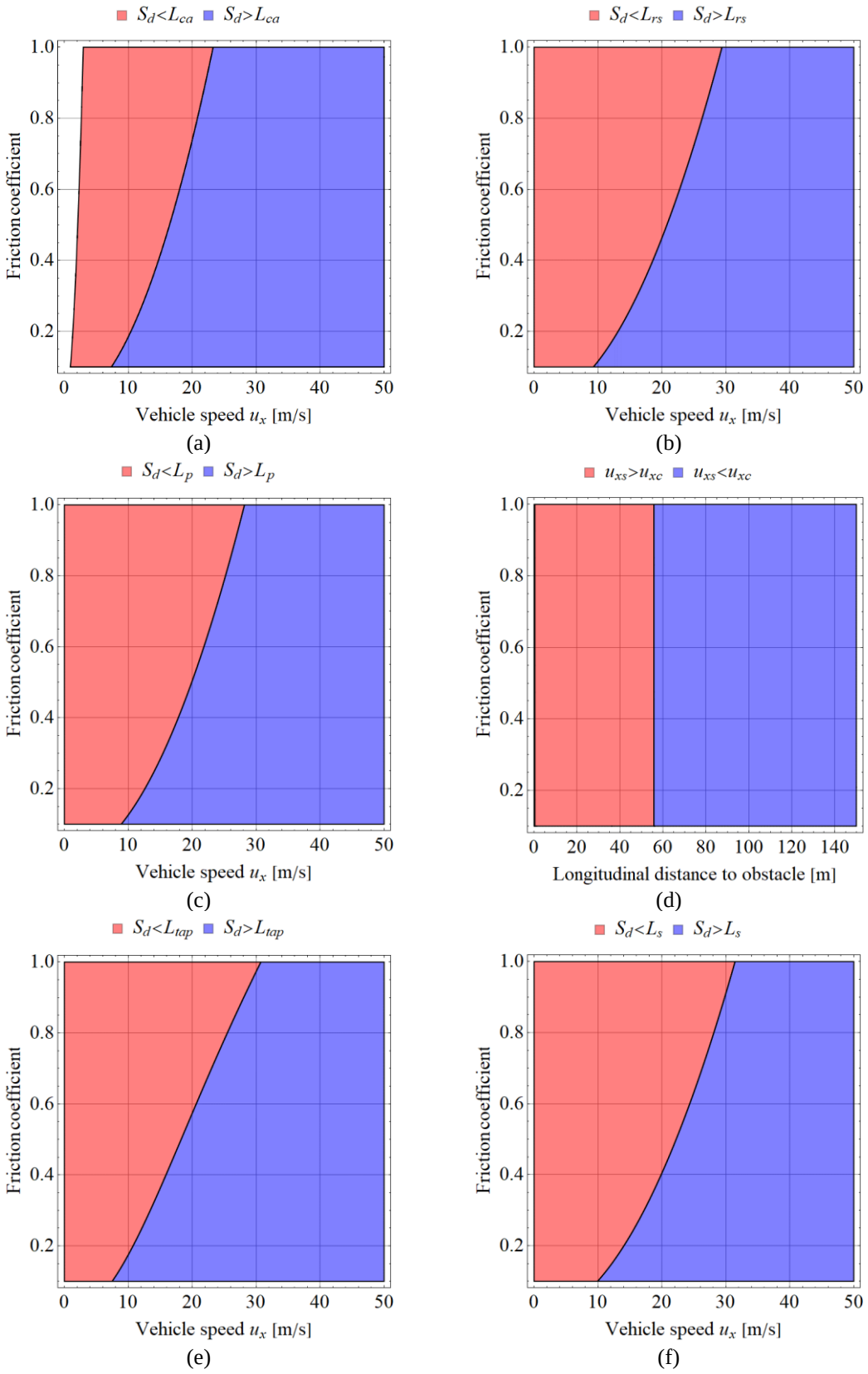

Figure 9: Regions in which either stopping or lane change maneuver gives the shortest longitudinal distance required to avoid the obstacle for (a) circular arcs, (b) ramp sinusoidal, (c) polynomial, (e) trapezoidal acceleration profile, and (f) sigmoid, or the maximum entry vehicle speed for (d) clothoid assuming a total lateral displacement of 3.5 m

ACKNOWLEDGEMENTS

The authors would like to acknowledge the support from the New Car Assessment Program for Southeast Asian Countries (ASEAN NCAP) through the ASEAN NCAP Collaborative Holistic Research – Phase III (ANCHOR III) research grant (No. A3-C391). This grant is registered at UTeM with the grant number ANTARABANGSA-ANCHOR/2020/FKM-CARE/A00029.

REFERENCES

Alleyne, A. (1997). A comparison of alternative intervention strategies for unintended roadway departure (URD) control. Vehicle System Dynamics, 27(3), 157-186.

Arbitmann, M., Stählin, U., Schorn, M., & Isermann, R. (2012). Method and device for performing a collision avoidance maneuver. United States Patent, US 8,209,090 B2.

Arikere, A., Yang, D., & Klomp, M. (2019). Optimal motion control for collision avoidance at left turn across path/opposite direction intersection scenarios using electric propulsion. Vehicle System Dynamics, 57(5), 637-664.

Chee, W., & Tomizuka, M. (1994). Lane change maneuver for AHS applications. International Symposium on Advanced Vehicle Control, 420-425.

Fors, V., Olofsson, B., & Nielsen L. (2020). Attainable force volumes of optimal autonomous at-the-limit vehicle manoeuvres. Vehicle System Dynamics, 58(7), 1101-1122.

Funke, J., & Gerdes, J.C. (2016). Simple clothoid lane change trajectories for automated vehicles incorporating friction constraints. Transactions ASME Journal of Dynamic Systems, Measurement, and Control, 138(2), 021002.

Gao, Y., Gordon, T., & Lidberg, M. (2019). Optimal control of brakes and steering for autonomous collision avoidance using modified Hamiltonian algorithm. Vehicle System Dynamics, 57(8), 1224-1240.

Goh, J.Y., Goel, T., & Gerdes, J.C. (2020). Toward automated vehicle control beyond the stability limits: drifting along a general path. Transactions ASME Journal of Dynamic Systems, Measurement, and Control, 142(2), 021004.

Gray, A., Gao, Y., Lin, T., Hedrick, J.K., Tseng, H.E., & Borrelli, F. (2012). Predictive control for agile semi-autonomous ground vehicles using motion primitives. American Control Conference, 4239-4244.

Isermann, R., Mannale, R., & Schmitt K. (2012). Collision-avoidance systems PRORETA: Situation analysis and intervention control. Control Engineering Practice, 20(11), 1236-1246.

Isermann, R., Schorn, M., & Stählin, U. (2008). Anticollision system PRORETA with automatic braking and steering. Vehicle System Dynamics, 46(S1), 683-694.

Kapania, N., & Gerdes, J.C. (2020). Learning at the racetrack: data-driven methods to improve racing performance over multiple laps. IEEE Transactions on Vehicular Technology, 69(8), 8232-8242.

Nelson, W. (1989). Continuous-curvature paths for autonomous vehicles. IEEE International Conference on Robotics and Automation, 1260-1264.

Shah, J., Best, M., Benmimoun, A., & Ayat, M.L. (2015). Autonomous rear-end collision avoidance using an electric power steering system. Proceedings of the Institution of Mechanical Engineers, Part D: Journal of Automobile Engineering, 229(12), 1638–1655.

Singh, A.S.P., & Nishihara, O. (2018). Nondimensionalized univariate equation characterizing optimal state feedback control for collision avoidance. IEEE Transactions on Intelligent Transportation Systems, 19(10), 3344-3359.

Singh, A.S.P., & Nishihara, O. (2020). Minimum resultant vehicle force optimal state feedback control for obstacle avoidance. IEEE Transactions on Control Systems Technology, 28(5), 1846-1861.

Singh, A.S.P., & Nishihara, O. (2021). Trajectory tracking and integrated chassis control for obstacle avoidance with minimum jerk. IEEE Transactions on Intelligent Transportation Systems. (early access)

Singh, A.S.P., Putra, A., & Kassim, K.A.A. (2020). Lane change and stopping maneuvers for emergency obstacle avoidance. 7th Mechanical Engineering Research Day, 30-31.

Singh, A.S.P., Putra, A., & Kassim, K.A.A. (2021). Time to collision for emergency obstacle avoidance. Journal of the Society of Automotive Engineers Malaysia, 5(2), 223-234.

Sledge, N.H., & Marshek, K.M. (1997). Comparison of ideal vehicle lane-change trajectories (No. 971062). SAE Technical Paper.

Soudbakhsh, D., Eskandarian, A., & Chichka, D. (2013). Vehicle collision avoidance maneuvers with limited lateral acceleration using optimal trajectory control. Transactions ASME Journal of Dynamic Systems, Measurement, and Control, 135(4), 041006.

Weber, D. (2012). Untersuchung des Potenzials einer Brems-Ausweich-Assistenz (Dissertation), Karlsruher Institut für Technologie, Germany.

Wilde, D. K. (2009). Computing clothoid segments for trajectory generation. IEEE/RSJ International Conference on Intelligent Robots and Systems, 2440-2445.

Yang, D, Jacobson, B., Jonasson, M, & Gordon, T.J. (2014). Closed-loop controller for post-impact vehicle dynamics using individual wheel braking and front axle steering. International Journal of Vehicle Autonomous Systems, 12(2), 158 – 179.

Yokoyama, A., Raksincharoensak, P., & Yoshikawa, N. (2018). Integrated steering and braking control system for collision avoidance by using virtual repulsive force field method. ASME Dynamic Systems and Control Conference, V002T22A001.

Yuan, H., Sun, X., & Gordon, T. (2019). Unified decision-making and control for highway collision avoidance using active front steer and individual wheel torque control. Vehicle System Dynamics, 57(8), 1188-1205.